Labyrinth Diode Designed by Topology Optimization of Binary Structures using Laminar Flow and Real Gas Properties with Experimental Validation

Lucas N. B. S. Ribeiro[1], Anderson S. C. Azevêdo[1], Renato Picelli[2] , Emílio C. N. Silva[1]

[1]*Dept. of Mechanical Engineering, University of São Paulo*
Av. Prof. Mello Moraes, 2231, Cidade Universitária, 05508-030 – São Paulo, Brazil
lucas.neves.ribeiro@usp.br, anderson.sca@usp.br, ecnsilva@usp.br
[2]*Dept. of Naval and Ocean Engineering*
Av. Prof. Mello Moraes, 2231, Cidade Universitária, 05508-030 – São Paulo, Brazil
rpicelli@usp.br

Abstract. One of the most pressing issues that require attention is the reduction of CO2 emissions, and one approach to mitigate this problem is by enhancing the performance of diodes used for sealing and minimizing leakage in turbomachinery. This study focuses on the design of a labyrinth diode using the Topology Optimization of Binary Structures (TOBS) method, which incorporates laminar flow and real gas properties. The labyrinth diode design is obtained through TOBS, considering energy dissipation and vorticity magnitude as a multi-objective framework within a specified volume fraction. The optimization problem takes into account the dimensions of the test bench and the properties of real CO2 gas in a two-dimensional axisymmetric model. The labyrinth diode design is optimized for laminar fluid flow governed by the Navier-Stokes equations, with the inclusion of the standard Darcy term to penalize solid domain infiltration. Computational Fluid Dynamics (CFD) is employed to numerically assess the diode's performance and compare it with experimental measurements, evaluating its effectiveness in reducing leakage. The optimized topology is transformed into a solid model and fabricated using UV-photosensitive resin through 3D printing. The fabricated prototype is then tested on a test bench (TB) equipped with a chamber capable of evaluating two seals with a middle entry, utilizing a 40 mm rotor. The TB can reach a maximum rotational speed of 10,000 rpm and generate a pressure drop of up to 5 bar. The leakage rate is measured in kg/s using instrumentation that adjusts the mass flow rate based on pressure/temperature analysis. The results indicate the need for further improvements to accommodate turbulent flow and higher Mach numbers in compressible flow during Topology Optimization. Nonetheless, the current findings offer promising insights into reducing leakage in turbomachinery seals.

Keywords: Topology Optimization, Labyrinth Diode, Laminar Flow, Experimental Validation

1 Introduction

Earth's temperature is regulated by the greenhouse effect and naturally occurring atmospheric greenhouse gases [1]). Post-Industrial Revolution, human activities escalated CO2, CH4, N2O, and F-gas emissions, intensifying warming [2]. Resulting in climate change challenges global governance [3]. Scientists stress emission reduction [2], evident in treaties like Kyoto Protocol and Paris Agreement. Notably, methane (CH4) with an energy absorption capacity 84 to 87 times greater than CO2, is a key contributor; in the US, 40% of 2019 emissions were from energy, 60% from natural gas systems [4], partially due to machinery leaks. Labyrinth seals help counter leakage, preserving fluid control. The labyrinth seals constitute a type of non-contact annular seal. They typically employ flow restrictions and cavities with the purpose of minimizing leakage or escape flow [5, 6]. The seal delineates a high-pressure region from a low-pressure one, and these regions can exist either between two stages of fluid machinery or between the internal and external regions of turbomachinery [7, 8].

When compared to other types of annular mechanical seals, labyrinth joints prevent friction between components, thereby contributing to an enhancement in the performance of fluid machinery [9]. Additionally, owing to their low cost, simple assembly, and high reliability, labyrinth seals constitute the majority of mechanical seals employed in turbomachinery [10–12], such as compressors, turbines, and turbochargers. There are a few test benches for experimental validation of Labyrinth Seals. It's possible to list some as the Turbomachinery Laboratory at Texas A&M University (shown in Fig.1(a)), which uses a Laser Doppler Anemometer (LDA) to measure the velocity field in the cavities of a Labyrinth Seal, or the Southeast University setup in China (shown in Fig. 1(b)) which measures the vibration effect duo different geometries labyrinth seals. Booth Test Benches are useful, but in this paper, we're interested only in leakage, pressure, and rotation conditions.

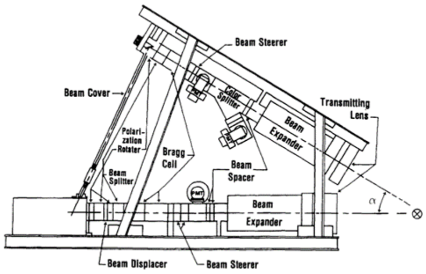

(a) Texas A&M University Labyrinth Seal Test Bench [13]

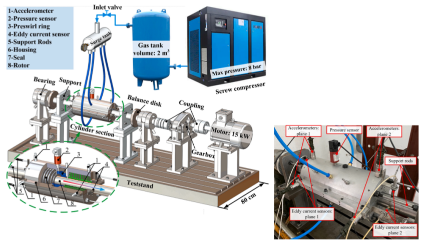

(b) Southeast University Labyrinth Seal Test Bench [14]

Figure 1. Labyrinth Seals Test Bench's List

Fluid flow Topology Optimization (TO) was introduced by Borrvall and Petersson [15] pursuing the path with minimum energy dissipation assuming a Stokes flow using continuous variables (or pseudo-densities approach). Ever since, TO has been also performed with other strategies like: level-set method [16], topological derivatives [17] and discrete (binary) variables [18]. Regarding the simulation complexity, fluid flow TO was employed to a variety of flow types extending the Stokes flow to: Navier-Stokes flow [19], swirling flows [20], and turbulent flows using κ-ϵ and κ-ω models [21]. These advances help engineers to design improved fluidic devices like: mixers, valves, machine rotors and Tesla-type turbines [22]. This paper's aim is to demonstrate a generic framework for manufacturing and test prototype designs of topology optimized labyrinth seals. The efficient generic mathematical programming of the TOBS method has shown potential for topology optimization computations for fluid flow applications (laminar regime [18], rotating flow [23], turbulent models [21] and subsonic compressibility effects [24]) using integer design variables. Therefore we chose this binary approach in order to obtain novel designs that reduce leakage in turbomachinery. Finally, the reliability of the design is verified, the prototype is manufactured using 3D printing and tested in a TB. The flow rate is compared at the same pressure and rotation conditions.

2 Fluid Flow Governing Equations for Topology Optimization

The fluid particles motion in a fluid domain Ω is modeled in the laminar regime assuming: i) constant density ρ and dynamic viscosity μ; ii) absolute velocity $\mathbf{v}$ and the pressure p fields independent of time; and iii) negligible body forces. Thus, the steady incompressible Navier-Stokes flow equations can be expressed as [25]:

$$\rho\left(\mathbf{v}\cdot\nabla\mathbf{v}\right) = -\nabla p + \mu\nabla^2\mathbf{v}, \tag{1}$$

$$\nabla\cdot\mathbf{v} = 0. \tag{2}$$

where Eq. 1 is the conservation of momentum and Eq. 2 is the continuity equations. Usually, fluid problem definitions include: the fluid entrance as the inlet (Γ_{in}); the exit as an outlet (Γ_{out}); and the solid frontier in inner flows as the fluid walls (Γ_{wall}). Herein, a fully developed inlet velocity profile, zero stress outlet, and no-slip conditions on fluid walls are adopted. The prescribed boundary conditions assumed are:

$$\mathbf{v} = \mathbf{v}_{in} \quad \text{on} \quad \Gamma_{in}, \tag{3}$$

$$-p\mathbf{I} + \nabla\mathbf{v}\cdot\mathbf{n} = \mathbf{0} \quad \text{on} \quad \Gamma_{out}, \tag{4}$$

$$\mathbf{v} = \mathbf{0} \quad \text{on} \quad \Gamma_{wall}, \tag{5}$$

where $\mathbf{v}_{in}$ is the average velocity on inlet, $\mathbf{I}$ is the identity matrix and $\mathbf{n}$ is the unit normal vector.

Classic fluid TO literature emulates solid regions as porous material with low permeability [15]. Therefore, a material model expression (Darcy term) must be added to the governing equation to emulate the regions in which the fluid is removed with resistance forces proportional to the velocity. In order to obtain the gradient data in solid and fluid domains on the discrete approach, the inverse permeability field $\kappa(\mathbf{x})$ for the design variable vector $\mathbf{x}$ is interpolated as the linear relation [18]:

$$\kappa(\mathbf{x}) = \kappa_{\max}\, x_{\mathrm{j}}, \tag{6}$$

in which x_j represents a set of binary design variables that indicate the presence of solid (x_j=1) or fluid (x_j=0) elements on the discretized design domain. This implies that only non-zeros design variables will have interpolated property equal to the assumed maximum inverse permeability value $\kappa_{\max}$. Thus, the laminar flow governing equation (Eq. 1) is rewritten as the generalized Navier-Stokes equations including the Darcy friction term:

$$\rho\left(\mathbf{v}\cdot\nabla\mathbf{v}\right) = -\nabla p + \mu\nabla^2\mathbf{v} - \kappa(\mathbf{x})\mathbf{v}. \tag{7}$$

3 Topology Optimization Problem

In order to solve the seal problem, boundary conditions were imposed on forward and backward flow directions. In these devices, the geometry can be designed to favor the flow in the desired direction while increasing the resistance on the opposite direction, similar to a Tesla valve [26]. However, the traditional expression used to maximize diodicity is susceptible to an undesired local minimum which closes the channel (creates a solid region that obstructs the flow path). Therefore we achieve the diodicity maximization by combining energy dissipation and vorticity on opposed flow directions (instead of the classical approach that uses only energy dissipation terms).

The fluid viscous energy dissipation $E(\mathbf{x})$ and the vorticity $\Phi(\mathbf{x})$ in the 2D-axisymmetric space can be expressed related to the radial coordinate $\mathbf{r}$ as:

$$E(\mathbf{x}) = \int_\Omega \left(\frac{\mu}{2}||\nabla\mathbf{v} + \nabla\mathbf{v}^T||^2 + \kappa(\mathbf{x})||\mathbf{v}||^2\right) 2\pi\mathbf{r}\, d\Omega, \tag{8}$$

$$\Phi(\mathbf{x}) = \int_\Omega ||\nabla\times\mathbf{v}||\; 2\pi\mathbf{r}\; d\Omega. \tag{9}$$

In this paper, we perform diodicity maximization by minimizing the forward energy dissipation E_{forw} while maximizing the backward vorticity Φ_{back} subjected to a fluid volume constraint $V(\mathbf{x})$. Therefore, the topology optimization problem is given by:

$$\begin{aligned} \underset{\mathbf{x}}{\text{Minimize}} \quad & F = w_1\cdot\log\left(E_{forw}(\mathbf{x})\right) - w_2\cdot\log\left(\Phi_{back}(\mathbf{x})\right) \\ \text{Subject to} \quad & V(\mathbf{x}) \le \overline{V}, \\ & x_j \in [0,1]. \end{aligned} \tag{10}$$

where $\overline{V}$ is the prescribed volume fraction, and w_1 and w_2 are weight parameters used to control the dominance of effects. We ensure the proportion $w_1 + w_2 = 1$.

3.1 Numerical Implementation

The TOBS method [27] is a viable option to solve the binary optimization problem. This methodology combines known ingredients in the optimization community, such as sensitivity analysis, numerical filtering, sequential integer linear programming (SILP) and a branch-and-bound solver. The TOBS method solves the binary optimization problem in the linearized form given by:

$$\begin{aligned} \underset{\Delta\mathbf{x}^k}{\text{Minimize}} \quad & \left.\frac{\partial f(\mathbf{x})}{\partial\mathbf{x}}\right|_{\mathbf{x}^k} \Delta\mathbf{x}^k \\ \text{Subject to} \quad & \left.\frac{\partial g_i(\mathbf{x})}{\partial\mathbf{x}}\right|_{\mathbf{x}^k} \Delta\mathbf{x}^k \le \bar{g}_i - g_i(\mathbf{x}^k) := \Delta g_i^k, \\ & \parallel \Delta x_j \parallel_1 \le \beta N_d, \\ & \Delta x_j \in \{-x_j, 1-x_j\}, \end{aligned} \tag{11}$$

where the linearized functions are obtained via the first order Taylor approximation. The term $g_i(\mathbf{x}^k)$ is the value of constraint g_i at iteration k of optimization. The truncation error constraint parameter β is employed to restrict the maximum flips (changes of discrete values for one state to another, e.g. 0 to 1 and vice versa) as a percentage of N_d and to ensure that the truncation error of the linearization approximation is sufficiently small. The infeasibility is avoided by relaxing the upper bounds constraints.

In this work, the problem is solved via a branch-and-bound algorithm implemented in CPLEX optimization library. The SILP solver is used to find the optimal change $\Delta\mathbf{x}$ for the integer design variables $\mathbf{x}$. After each iteration, the design variables are updated as $\mathbf{x}^{k+1} = \mathbf{x}^k + \Delta\mathbf{x}^k$. Full details and an educational code is given by Picelli et al. [28]. The convergence is evaluated in two steps. First, we compute the average of the objective function F changes over $2\ N$ consecutive iterations. After the first convergence, we update the $\kappa_{\max}$ values for the continuation approach. Then, the changes between design variables state from the current converged topology at iteration k_z and the previous converged topology at k_{z-1} are verified. Therefore the convergence criteria are:

$$error_1 = \frac{\sum_{i=1}^{N}(F_{k-i+1} - F_{k-N-i+1})}{\sum_{i=1}^{N} F_{k-i+1}} \leq \tau_1 \quad \text{and} \quad error_2 = \frac{\sum_{j=1}^{N_d} |x_j^{k_z} - x_j^{k_{z-1}}|}{N_d} \leq \tau_2, \tag{12}$$

where k represents the current iteration number, τ_1 and τ_2 are respectively the objective and design variables tolerance errors. If this latter criterion was not satisfied until an allowed value for $\kappa_{\max}$ the optimization stops.

A regular mesh of quadrilateral elements is adopted for both flow directions assuming respectively quadratic and linear basis for velocity and pressure fields. Sensitivity computation is performed via automatic differentiation. This procedure was implemented in COMSOL Multiphysics ® LiveLink with MATLAB®. Figure 2 illustrates the optimization procedure adopted.

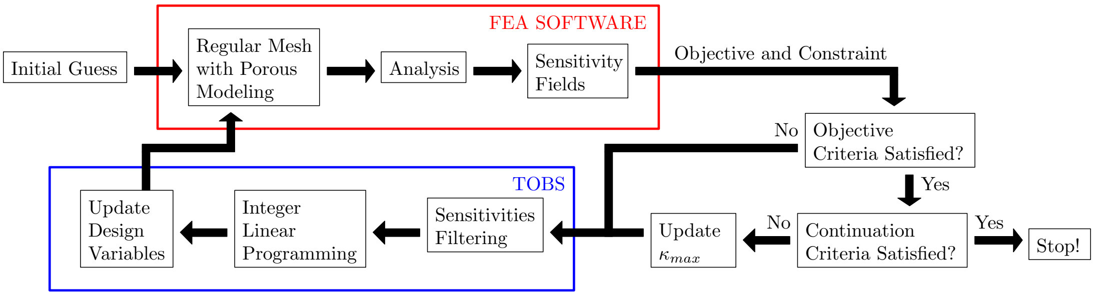

Figure 2. General framework of TOBS for the seal problem.

4 Numerical Result

This section presents an example in which fluid flows through the axisymmetric labyrinth seal with aligned entrances entering with a fully developed velocity profile boundary condition and exiting with reference pressure $p_{out} = 0$ Pa. It was assumed a fully fluid initial guess. The TO problem is expressed in Eq. 10 considering $\overline{V} = 0.6$. It is assumed Re = 150 on each flow direction and a 75×245 elements optimization grid is used. The continuation scheme starts with $\kappa_{\max} = 1 \cdot 10^4$ kg/m^3·s and increases by 10^4 up to $2 \cdot 10^5$ kg/m^3·s with $\tau_1 = 0.0005$ and $\tau_2 = 0.025$. Figure 3 presents the analysis domain for forward (remarked in blue) and backward (remarked in red) flow. We denote as backward the direction of the flow that comes from the compressor and exits at the atmosphere. The length of the chamber corresponds to half of the TB size for simplicity.

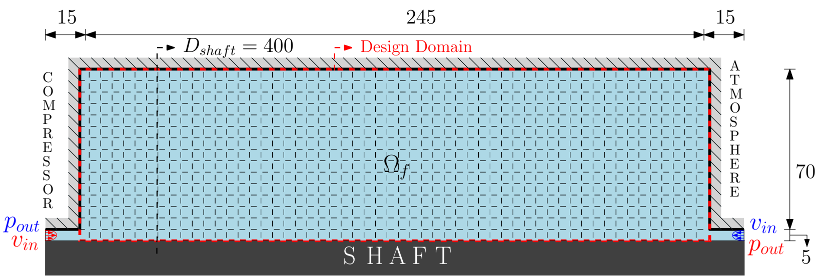

Figure 3. The seal problem boundary conditions for forward and backward flow. Units in mm.

Figure 4 presents the topology obtained after the optimization procedure and the solution of the velocity field at the direction that was designed to impose higher resistance to the flow. In order to show only the flow at the designed fluid path, we performed post-processing of the topology boundaries to smooth the staircase contour. Observe that the seal design favored the emergence of two recirculating regions. These interlaced vortices chambers contribute to making a long path to dissipate more energy on the seal mechanism.

After getting this result, a full geometry for the test bench has been done, coupling two TO results in series. With that geometry, a simulation was made using ANSYS Fluent®, with compressible and turbulent flow, using

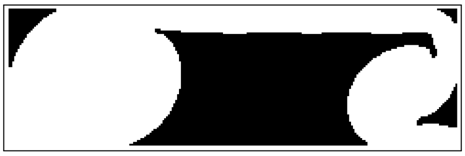

(a) Optimized topology for seal design chamber

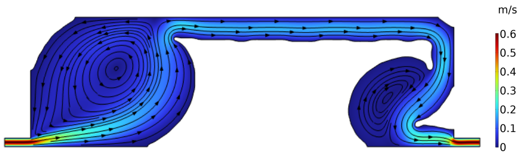

(b) Velocity field on backward flow

Figure 4. Solution of the topology optimization of the seal problem.

K- ωSST turbulence model, in a 2D-axisymmetric swirl flow domain, stationary (Pseudo-Transient), with real gas properties (Soave-Redlich-Kwong air model). The Pressure and Velocity results are shown in Fig. 5.

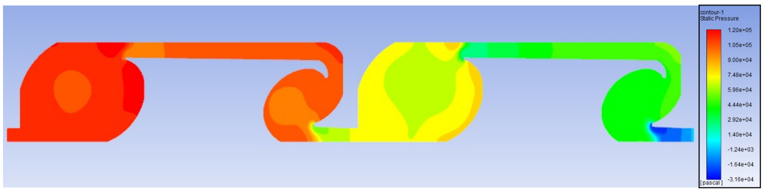

(a) Pressure Field

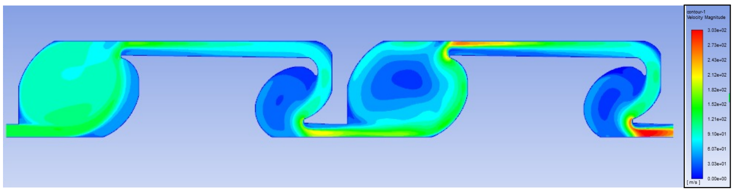

(b) Velocity Field

Figure 5. Compressible Turbulent Flow CFD results

5 Prototype Manufacturing for Experimental Validation

The first step is to convert the TO result into a CAD file. For this task, it's used the software SOLIDWORKS® to create a sketch extracted from the design domain and then revolutionize it, generating volumetric bodies. The stator was divided into two parts with pins for guided assembly. Utilizing Halot Box® software, the printable file was obtained and used to produce the prototype on a Creality Halot Sky 3D printer. This printer uses UV-cured grey resin with a 4K resolution 9.25" screen, ensuring high-quality layering at 0.05 mm height. Post-printing, parts underwent a 10-minute external cure in two different orientations. The labyrinth diode prototype's manufacturing steps and final assembly are illustrated in Fig. 6.

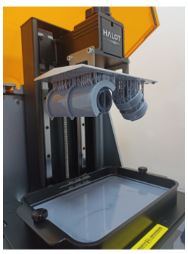

(a) 3D Printing process

(b) UV external cure

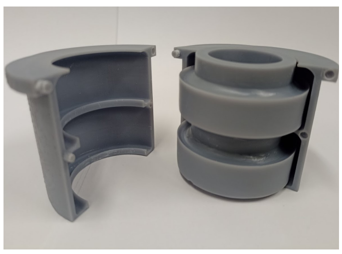

(c) Labyrinth Seal Assembly

Figure 6. Manufacture Process

The printed Labyrinth Seals are tested in our Test Bench at USP. The Test Bench is equipped with a chamber capable of evaluating two seals with a middle entry, utilizing a 40 mm rotor. The setup can reach a maximum rotational speed of 10,000 rpm and generate a pressure drop of up to 5 bar. The leakage rate is measured in kg/s using instrumentation that adjusts the mass flow rate based on pressure/temperature analysis, also shown in Fig 7.

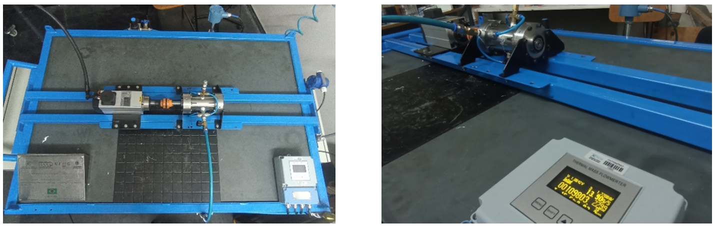

(a) Test Bench Overview (b) Measure Instrumentation

Figure 7. Labyrinth Seal Test Bench at USP

The Test Bench, along with the CFD analysis, is currently undergoing calibration. The current experimental results for the traditional Labyrinth Seal (baseline) are shown in Fig. 8. The distance between the results is evident, yet it remains a calibration and testing time issue. Moreover, tests will be conducted using the TO Labyrinth Seal to compare leakage and validate the effectiveness of the TO methodology.

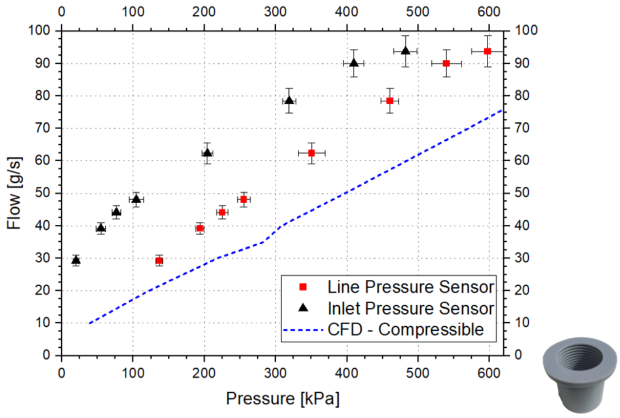

Figure 8. Experimental Results and CFD

6 Conclusion

This paper proposed a general framework for manufacturing prototypes with optimized designs is proposed by using additive manufacturing equipment. The Topology optimized design was obtained considering a simplified flow condition in the two-dimensional axisymmetric model assuming laminar incompressible CO2 in realistic test bench dimensions. The CFD is used to guide experimental validation but is still under parameters calibration to get closer to the experimental. The proposed framework to manufacture the Labyrinth Seal using addictive manufacture has proven efficient. The Measuring process looks nice and efficient, but still a work in progress, under calibration. The proposed analysis serves as a recommendation for future works on verifying and prototyping optimized labyrinth fluid diodes. Topology Optimization for test bench pressure conditions and experimental comparison of performance with baseline seals are future directions of this research.

Acknowledgements. L.N.B.S. Ribeiro and A.S.C. Azevêdo thank the financial support of FUSP (University of São Paulo Foundation) project number 371065. R. Picelli would like to thank the support of FAPESP, grants 2018/05797-8 and 2019/01685-3. E.C.N. Silva thanks the financial support of CNPq (National Council for Research and Development) under grant 302658/2018-1. We gratefully acknowledge support of the RCGI – Research Centre for Greenhouse Gas Innovation, hosted by the University of São Paulo (USP) and sponsored by FAPESP (2014/50279-4 and 2020/15230-5) and Shell Brasil, and the strategic importance of the support given by ANP (Brazil's National Oil, Natural Gas and Biofuels Agency) through the R&D levy regulation.

Authorship statement. The authors hereby confirm that they are the sole liable persons responsible for the authorship of this work, and that all material that has been herein included as part of the present paper is either the property (and authorship) of the authors, or has the permission of the owners to be included here.

References

[1] EPA. Overview of greenhouse gases. Technical report, United States Environmental Protection Agency, 2021.
[2] IPCC. Climate report. Technical report, International Panel of Climate Changes, 2021.
[3] A. C. Santos and A. N. Pontes. EmissÕes de gases de efeito estufa e mudanÇas climÁticas no estado do parÁ. *Educamazônia-Educação,Sociedade e Meio Ambiente*, vol. 15, 2022.
[4] EPA. Inventory of united states. Technical report, United States Environmental Protection Agency, 2019.
[5] A. J. Macintyre. *Máquinas Motrizes Elétricas*. Guanabara Dois SA., 1983.
[6] H. Sneck. Labyrinth seal literature survey. *Journal of Tribology*, vol. 96, 2004.
[7] C. Pfleiderer and H. Petermann. *Máquinas de Fluxo*. Livros Técnicos e Científicos, 1979.
[8] Y. Dereli and D. Eser. Flow calculations in straight-through labyrinth seals by mathematical and computational applications. *Association for Scientific Research 9*, vol. 9, 2004.
[9] D. W. Childs and J. M. Vange. Annular gas seals and rotordynamics of compressors and turbines, 1997.
[10] B. M. Steinetz and R. C. Hendricks. Engine seal technology requirements to meet nasa's advanced subsonic technology program goals. volume 30, 1996.
[11] H. ZHANG, X. JIA, X. PAN, and Q. I. B.and ZHENG. JIANG. Interaction between rotor and annular seals: interlaced and straight-through labyrinth seals. *Journal of Propulsion and Power*, vol. 32, 2016.
[12] G. ILIEVA and C. PIROVSKY. Labyrinth seals with application to turbomachinery. *Materialwissenschaft und Werkstofftechnik*, vol. 50, 2016.
[13] G. L. Morrison, M. C. Johnson, R. E. DeOtte, H. Davis Thames, and B. G. Wiedner. An experimental technique for performing 3d lda measurements inside whirling annular seals. *Flow Measurement and Instrumentation*, vol. 5, n. 1, pp. 43–49, 1994.
[14] Q. Gu, J. Yang, W. Zhang, and M. Zhang. On the dynamic performance of a novel airfoil guider seal with the controlled circumferential flow: Numerical analysis and experimental validation. *Tribology International*, vol. 167, pp. 107413, 2022.
[15] T. Borrvall and J. Petersson. Topology optimization of fluids in Stokes flow. *International Journal for Numerical Methods In Fluids*, vol. 41, pp. 77–107, 2003.
[16] X. Duan, F. Li, and X. Qin. Topology optimization of incompressible navier-stokes problem by level set based adaptive mesh method. *Computers & Mathematics with Applications*, vol. 72, n. 4, pp. 1131–1141, 2016.
[17] L. F. N. Sá, R. C. R. Amigo, A. A. Novotny, and E. C. N. Silva. Topological derivatives applied to fluid flow channel design optimization problems. *Structural and Multidisciplinary Optimization*, vol. 54, n. 2, pp. 249–264, 2016.
[18] B. Souza, P. V. M. Yamabe, L. F. N. Sá, S. Ranjbarzadeh, R. Picelli, and E. C. N. Silva. Topology optimization of fluid flow by using integer linear programming. *Structural and Multidisciplinary Optimization*, vol. 64, pp. 1221–1240, 2021.
[19] L. H. Olesen, F. Okkels, and H. Bruus. A high-level programming-language implementation of topology optimization applied to steady-state navier-stokes flow. *International Journal for Numerical Methods in Engineering*, vol. 65, n. 7, pp. 975–1001, 2006.
[20] D. H. Alonso, L. F. N. Sá, J. S. R. Saenz, and E. C. N. Silva. Topology optimization applied to the design of 2d swirl flow devices. *Structural and Multidisciplinary Optimization*, vol. 58, pp. 2341–2364, 2018.
[21] R. Picelli, E. Moscatelli, P. V. M. Yamabe, D. H. Alonso, S. Ranjbarzadeh, R. S. Gioria, and J. R. M. E. C. N. Silva. Topology optimization of turbulent fluid flow via the tobs method and a geometry trimming procedure. *Structural and Multidisciplinary Optimization*, vol. 65: 34, 2022.
[22] D. H. Alonso and E. C. N. Silva. Topology optimization applied to the design of tesla-type turbine devices. *Applied Mathematical Modelling*, vol. 103, pp. 764–791, 2022.
[23] E. Moscatelli, D. H. Alonso, L. F. N. Sá, R. Picelli, and E. C. N. Silva. Topology optimisation for rotor-stator fluid flow devices. *Structural and Multidisciplinary Optimization*, vol. 65: 142, 2022.
[24] F. S. Maffei, L. F. Nogueira de Sá, E. Moscatelli, R. Picelli, J. R. Meneghini, and E. C. Nelli Silva. Integer programming topology optimization for subsonic compressible flows with geometry trimming. *International Journal of Heat and Mass Transfer*, vol. 201, pp. 123614, 2023.
[25] F. M. White. *Fluid Mechanics*. Mc Graw Hill, 7th edition, 2011.
[26] S. Lin, L. Zhao, J. K. Guest, T. P. Weihs, and Z. Liu. Topology Optimization of Fixed-Geometry Fluid Diodes. *Journal of Mechanical Design*, vol. 137, n. 8, 2015.
[27] R. Sivapuram and R. Picelli. Topology optimization of binary structures using integer linear programming. *Finite Elements in Analysis and Design*, vol. 139, pp. 49–61, 2018.
[28] R. Picelli, R. Sivapuram, and Y. M. Xie. A 101-line MATLAB code for topology optimization using binary variables and integer programming. *Structural and Multidisciplinary Optimization*, vol. Online september 2020, pp. 1–20, 2020.